International Journal of Heat and Fluid Flow 30 (2009) 902–910

Contents lists available at ScienceDirect

International Journal of Heat and Fluid Flow

journal homepage: www.elsevier.com/locate/ijhff

Double diffusive natural convection in a partially heated enclosure with Soret and Dufour effects

N. Nithyadevi, Ruey-Jen Yang *

Department of Engineering Science, National Cheng Kung University, Tainan 70101, Taiwan, ROC

ARTICLE INFO

Article history:
Received 25 August 2008
Received in revised form 2 April 2009
Accepted 3 April 2009
Available online 8 May 2009

Keywords:
Double-diffusive natural convection
Square enclosure
Control volume method
Soret and Dufour effects

ABSTRACT

The effect of double-diffusive natural convection of water in a partially heated enclosure with Soret and Dufour coefficients around the density maximum is studied numerically. The right vertical wall has constant temperature θ_c, while left vertical wall is partially heated θ_h, with $\theta_h > \theta_c$. The concentration in right wall is maintained higher than left wall ($C_c < C_h$) for case I, and concentration is lower in right wall than left wall ($C_h > C_c$) for case II. The remaining left vertical wall and the two horizontal walls are considered adiabatic. Water is considered as the working fluid. The governing equations are solved by control volume method using SIMPLE algorithm with QUICK scheme. The effect of the various parameters (thermal Rayleigh number, center of the heating location, density inversion parameter, Buoyancy ratio number, Schmidt number, and Soret and Dufour coefficients) on the flow pattern and heat and mass transfer has been depicted. Comprehensive Nusselt and Sherwood numbers data are presented as functions of the governing parameters mentioned above.

1. Introduction

The natural convection in enclosures continues to be a very active area of research during the past few decades. While a good number of works have made significant contributions for the development of the theory, an equally good number of works have been devoted to many engineering applications that include electronic or computer equipment, thermal energy storage systems and etc. For a detailed survey of literature on the natural convection heat transfer may look at Davis (1983) and Ostrach (1988). However, we shall refer to a few important works that may serve as background for the present work.

In most of the analysis pertaining to the convection of water in enclosures, a linear temperature density relationship was taken. But in practice this will never happen as the density of water varies with temperature in a nonlinear fashion, attaining its maximum density around 4 °C. Nansteel et al. (1987) numerically studied the convection of cold water in the density maximum in a rectangular enclosure. Coupling of natural convection flow across a vertical density inversion is studied by Tong and Koster (1993). The numerical results reveal that the dominant convection is determined by the horizontal location of the maximum density plane. The penetration is highest at small Rayleigh numbers. Transient flow field and heat transfer behavior of cold water in an enclosure is numerically investigated by Chang and Yang (1995). Ho and Tu (2001) also studied transient flow of water. Osorio et al. (2004) studied experimentally and numerically the natural convection of water near its density inversion in a square enclosure.

Double diffusive convection of water has been studied by Sezai and Mohamad (2000) and Sivasankaran and Kandaswamy (2006, 2007). Yet, most work done considers flow inside closed enclosures, the applications included, such as pollution dispersion in lakes, chemical deposition, and melting and solidification process. In most of the problems, Soret and Dufour effects are assumed to be negligible. But the present work investigates both effects. Diffusion of matter caused by temperature gradients (Soret effect) and diffusion of heat caused by concentration gradients (Dufour effect) become very significant when the temperature and concentration gradients are very large. Generally these effects are considered as second order phenomenon. In the effects may become important in some applications such as the solidification of binary alloys, groundwater pollutant migration, chemical reactors, and geosciences. The importance of these effects has also seen in Joly et al. (2000), Bahloul et al. (2003), Mansour et al. (2006), Patha et al. (2006) and Platten (2006).

Joly et al. (2000) made the Soret effect on natural convection in a vertical enclosure. They analyzed the particular situation where the buoyancy forces induced by the thermal and solutal effects are opposing each other and of equal intensity. Double diffusive and Soret induced convection in a shallow horizontal enclosure is analytically and numerically studied by Bahloul et al. (2003) and also studied numerically by Mansour et al. (2006). They found that the Nusselt number has decreases in general with the Soret

* Corresponding author. Tel.: +886 6 2002724; fax: +886 6 2766549.
E-mail address: rjyang@mail.ncku.edu.tw (R.-J. Yang).

0142-727X/$ - see front matter © 2009 Elsevier Inc. All rights reserved.
doi:10.1016/j.ijheatfluidflow.2009.04.001

Nomenclature

Alphabetics

C	dimensional concentration (kg m^{-3})
c_p	specific heat at constant pressure (J kg^{-1} K^{-1})
c_s	concentration susceptibility
D	solutal diffusivity (m^2 s^{-1})
D_f	Dufour parameter
D_m	constant molecular diffusivity(m^2 s^{-1})
G	acceleration due to gravity (ms^{-2})
k_T	thermal diffusion ratio
L	length of the cavity (m)
Nu	local Nusselt number
$\overline{Nu}$	average Nusselt number
P	pressure (kg m^{-1} s^{-2})
Pr	Prandtl number
R	dimensionless density inversion parameter
Ra_C	solutal Rayleigh number
Ra_T	thermal Rayleigh number
Sc	Schmidt number
Sh	local Sherwood number
$\overline{Sh}$	average Sherwood number
S_r	Soret parameter
t	dimensional time (s)
T	dimensionless temperature
u,v	velocity components (m s^{-1})
U,V	dimensionless velocity components
x,y	dimensional coordinates (m)
X,Y	dimensionless coordinates
W	center of the heating location (m)

Greek symbols

α	thermal diffusivity (m^2 s^{-1})
β_T	coefficient of thermal expansion (K^{-2})
β_C	coefficient of solutal expansion (m^3 kg^{-1})
μ	dynamic viscosity (kg m^{-1} s^{-1})
ν	kinematic viscosity (m^2 s^{-1})
θ	temperature (K)
θ_I	temperature at maximum density (K)
θ_m	mean fluid temperature (K)
ρ	density (kg m^{-3})
τ	dimensionless time

Subscripts

c	cold wall
h	hot wall
o	reference state

parameter while the Sherwood number increases or decreases with this parameter depending on the temperature gradient induced by each solution.

In the above studies convection heat transfer is due to the imposed temperature gradient between the opposing walls of the enclosure taking the entire vertical wall to be thermally active. But in many naturally occurring situations and engineering applications it is only a part of the wall which is thermally active. For example in solar energy collectors due to shading, it is only the unshaded part of the wall that is thermally active. In order to have the results to possess applications, it is essential to study heat transfer in an enclosure with partially heated active walls. Only a few studies are reported in the literature concerning heat transfer in enclosures with partially heated side walls, by Valencia and Frederick (1989), Yucel and Turkoglu (1994), Frederick and Quiroz (2001), Erbay et al. (2004) and Oztop (2007).

Natural convection in an enclosure with partially active walls is studied by Nithyadevi et al. (2006, 2007) and Kandaswamy et al. (2007) without Soret and Dufour effects. Present study deals with the natural convection in a square enclosure filled with water and partially heated vertical walls for three different combinations of heating location in the presence of solute concentration with Soret and Dufour effects. The hot region is located at the top, middle and bottom of the left vertical wall of the enclosure.

2. Mathematical formulation

The unsteady two-dimensional natural convection flow in a square enclosure of length L filled with water is considered as shown in Fig. 1. The partially heated active vertical left side wall ($h = L/2$) and fully heated active vertical right side wall of the enclosure are maintained at two different but uniform temperatures and concentrations, namely, θ_h and θ_c, c_c and c_h (case I) or c_h and c_c (case II), with $\theta_h > \theta_c$ and $c_h > c_c$, respectively. The remaining boundaries of the enclosure are thermally insulated. The heat and mass transfer characteristics are investigated for three different combinations of the heated active wall (viz.), the hot location moving from top to bottom of the left wall. The gravity acts normal to the x-axis. The velocity components u and v are taken in the x and y directions, respectively. Under the above assumptions, the conservation equations of mass, momentum, energy and concentration with the Soret and Dufour effects in a two-dimensional Cartesian co-ordinate system are

$$\frac{\partial u}{\partial x}+\frac{\partial v}{\partial y}=0, \tag{1}$$

$$\frac{\partial u}{\partial t}+u\frac{\partial u}{\partial x}+v\frac{\partial u}{\partial y}=-\frac{1}{\rho_0}\frac{\partial p}{\partial x}+\nu\nabla^2 u \tag{2}$$

$$\frac{\partial v}{\partial t}+u\frac{\partial v}{\partial x}+v\frac{\partial v}{\partial y}=-\frac{1}{\rho_0}\frac{\partial p}{\partial y}+\nu\nabla^2 v-\frac{\rho}{\rho_0}g \tag{3}$$

$$\frac{\partial \theta}{\partial t}+u\frac{\partial \theta}{\partial x}+v\frac{\partial \theta}{\partial y}=\alpha\nabla^2\theta+\frac{Dk_T}{c_s c_p}\nabla^2 c \tag{4}$$

$$\frac{\partial c}{\partial t}+u\frac{\partial c}{\partial x}+v\frac{\partial c}{\partial y}=D\nabla^2 c+\frac{Dk_T}{\theta_m}\nabla^2\theta \tag{5}$$

The following assumptions are considered. The density of the cold water is assumed to vary with temperature according to the following parabolic relationship as Tong and Koster (1993): $\rho = \rho_o[1-\beta_T(\theta-\theta_I)^2]$, where ρ_o is the maximum density at the temperature $\theta_I = 3.98$ °C. This variation, due to both temperature

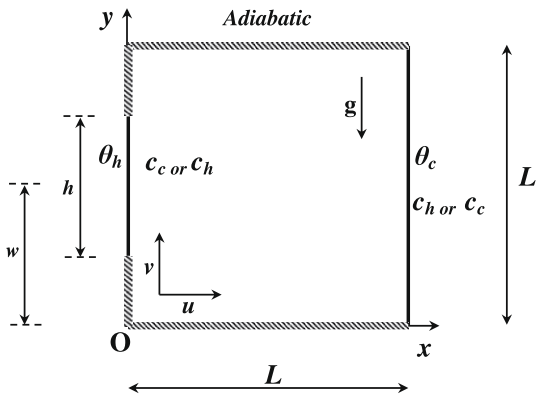

Fig. 1. Physical configuration.

and concentration gradients, can be described by the following equation $\rho = \rho_o[1 - \beta_T(\theta - \theta_l)^2 + \beta_C(c - c_o)]$, ($\beta_T = 8.0 \times 10^{-6}$(°C) K^{-2}, $\beta_C = 3.0 \times 10^{-3}$ m^3 kg^{-1}) where β_T and β_C are the coefficients for thermal and concentration expansions.

The appropriate initial and boundary conditions are:

$$t = 0: \quad u = v = 0, \quad \theta = \theta_c, \quad c = c_c, \quad 0 \leqslant x \leqslant L, \quad 0 \leqslant y \leqslant L,$$

$$t > 0: \quad u = v = 0, \quad \frac{\partial \theta}{\partial y} = \frac{\partial c}{\partial y} = 0, \quad 0 \leqslant x \leqslant L, \quad y = 0 \ \& \ L,$$

$$\theta = \theta_h, \quad c = c_c \text{ or } c_h, \quad x = 0, \quad w - \frac{h}{2} \leqslant y \leqslant w + \frac{h}{2}, \quad \theta = \theta_c,$$

$$c = c_h \text{ or } c_c, \quad x = L, \quad 0 \leqslant y \leqslant L, \quad \frac{\partial \theta}{\partial x} = \frac{\partial c}{\partial x} = 0, \quad x = 0,$$

$$0 \leqslant y \leqslant w - \frac{h}{2}, \quad w + \frac{h}{2} \leqslant y \leqslant L.$$

Introducing the following non-dimensional variables

$$\tau = \frac{t}{L^2/\nu}, \quad (X, Y) = \frac{(x, y)}{L}, \quad (U, V) = \frac{(u, v)}{\nu/L}, \quad P = \frac{pL^2}{\rho_0 \nu^2},$$

$$W = \frac{w}{L}, \quad T = \frac{\theta - \theta_c}{\theta_h - \theta_c}, \quad C = \frac{c - c_c}{c_h - c_c}, \text{ with } \theta_h > \theta_c, \quad c_h > c_c.$$

The non-dimensional form of the Eqs. (1)–(5) are obtained as,

$$\frac{\partial U}{\partial X} + \frac{\partial V}{\partial Y} = 0, \tag{6}$$

$$\frac{\partial U}{\partial \tau} + U\frac{\partial U}{\partial X} + V\frac{\partial U}{\partial Y} = -\frac{\partial P}{\partial X} + \nabla^2 U \tag{7}$$

$$\frac{\partial V}{\partial \tau} + U\frac{\partial V}{\partial X} + V\frac{\partial V}{\partial Y} = -\frac{\partial P}{\partial Y} + \nabla^2 V + \frac{Ra_T}{\mathrm{Pr}}[(T - R)^2 - NC] \tag{8}$$

$$\frac{\partial T}{\partial \tau} + U\frac{\partial T}{\partial X} + V\frac{\partial T}{\partial Y} = \frac{1}{\mathrm{Pr}}\nabla^2 T + D_f \nabla^2 C \tag{9}$$

$$\frac{\partial C}{\partial \tau} + U\frac{\partial C}{\partial X} + V\frac{\partial C}{\partial Y} = \frac{1}{Sc}\nabla^2 C + S_r \nabla^2 T \tag{10}$$

The initial and boundary conditions in the dimensionless form are:

$$\tau = 0: \quad U = V = 0, \quad T = C = 0, \quad 0 \leqslant X \leqslant 1, \quad 0 \leqslant Y \leqslant 1,$$

$$\tau > 0: \quad U = V = 0, \quad \frac{\partial T}{\partial Y} = \frac{\partial C}{\partial Y} = 0, \quad 0 \leqslant X \leqslant 1, \quad Y = 0 \ \& \ 1,$$

$$T = 1, \quad C = 0 \text{ or } 1, \quad X = 0, \quad W - \frac{1}{4} \leqslant Y \leqslant W + \frac{1}{4}, \quad T = 0,$$

$$C = 1 \text{ or } 0, \quad X = 1, \quad 0 \leqslant Y \leqslant 1, \quad \frac{\partial T}{\partial X} = \frac{\partial C}{\partial X} = 0, \quad X = 0,$$

$$0 \leqslant Y \leqslant W - \frac{1}{4}, \quad W + \frac{1}{4} \leqslant Y \leqslant 1.$$

The nondimensional parameters that appear in the equations are, $Ra_T = \frac{g\beta_T(\theta_h - \theta_c)^2 L^3}{\nu^2}$ thermal Rayleigh number, $Ra_c = \frac{g\beta_c(c_h - c_c)L^3}{\nu^2}$ solutal Rayleigh number, $\mathrm{Pr} = \frac{\nu}{\alpha} = 11.573$ Prandtl number, $D_f = \frac{Dk_T(c_h - c_c)}{c_s c_p \nu(\theta_h - \theta_c)}$ Dufour parameter, $S_r = \frac{Dk_T(\theta_h - \theta_c)}{\theta_m \nu(c_h - c_c)}$ Soret parameter, $Sc = \frac{\nu}{D}$ Schmidt number, $R = \frac{\theta_l - \theta_c}{\theta_h - \theta_c}$ density inversion parameter, and $N = \frac{Ra_c}{Ra_T}$ Buoyancy ratio number.

The local Nusselt number and Sherwood number is defined by $Nu = -\frac{\partial T}{\partial X}|_{X=0}$, $Sh = -\frac{\partial C}{\partial X}|_{X=1}$, or $-\frac{\partial C}{\partial X}|_{X=0}$, resulting in the average Nusselt number and Sherwood number as $\overline{Nu} = \frac{1}{h}\int_h Nu\, dY$, $\overline{Sh} = \int_0^1 Sh\, dY$ or $\frac{1}{h}\int_h Sh\, dY$, where $h = \frac{L}{2}$ is height of heating location.

3. Method of solution

The governing equations reported in the previous section are solved numerically using SIMPLE algorithm of Patankar (1980). The discretizations followed the QUICK scheme. This method, based on the control volume formulation, is appropriate for working with mixed boundary conditions and for the treatment of the pressure-velocity coupling. The resulting set of discretized equations for each variable is solved by a line-by-line procedure, combining the tri-diagonal matrix algorithm (TDMA). Under relaxation technique is employed for the pressure correction. The mass balance for global convergence is taken as 10^{-7}. Uniform staggered grid system is employed in the present study. The average Nusselt numbers for various grid sizes (21×21 to 91×91) are presented to develop an understanding of the grid fineness that is necessary for accurate numerical simulation as seen in Fig. 2. There is considerable change in the average Nusselt number from 21×21 to 51×51 and no noticeable change is observed from 51×51 to 91×91. Hence considering the accuracy of the results required and computational time involved a 51×51 grid size is chosen for all computational. The comparison of the calculated average Nusselt number using the present numerical method for different Rayleigh numbers with literature is presented by Nithyadevi and Yang (2009). Relatively good agreement is obtained. We are, therefore, confident that the results reported in our paper are accurate.

4. Results and discussion

In the studied configuration, double diffusive natural convection of water in a two-dimensional partially heated enclosure in the presence of Soret and Dufour effects around the region of its density maximum. The computations are carried out for different values of thermal Rayleigh number, Buoyancy ratio number, Density inversion parameter, Schmidt number, Soret parameter and Dufour parameter with different heating locations. The parameters considered are in the range $10^3 \leqslant Ra_T \leqslant 10^6$ (thermal Rayleigh number), $0.8 \leqslant N \leqslant 1.2$ (Buoyancy ratio number), $0 \leqslant R \leqslant 2$ (Density inversion parameter), $1 \leqslant Sc \leqslant 5$ (Schmidt number), $0 \leqslant S_r \leqslant 1$ (Soret parameter), $0 \leqslant D_f \leqslant 1$ (Dufour parameter). The results are presented in the form of streamlines, isotherms, isoconcentration and mid-height velocity profiles to show the fluid flow, heat and mass transfer phenomena in transient and steady states. The rate of heat and mass transfer in the enclosure is measured in terms of the average Nusselt number and average Sherwood number.

At time $\tau = 0$, the fluid contained in the entire enclosure is homogeneous and at 0 °C and does not generate heat internally. For $\tau > 0$, the left heated active wall temperature is changed to θ_h and that of right wall is maintained at $\theta_c = 0$ °C = 273 K while in the left active concentration wall C_c and right wall C_h (case I) or left wall C_h and the right one C_c (case II) with Soret parameter $S_r = 1$. Since the temperature of the left wall is higher than that of the fluid inside the cavity, the wall transmits heat to the fluid by conduction and raises the temperature of fluid particles adjoining the left wall.

Fig. 3a–h shows the evolution of fluid motion and subsequent distribution of heat and mass across the enclosure as time evolves. The results for transient state regime in case I are presented for thermal Rayleigh number $Ra_T = 10^5$ with $N = 1$, $R = 0.5$, $Sc = 5$, $S_r = 1.0$ and $D_f = 0.0$ as a representative case. A weak convective counter rotating cells appeared along the isothermal walls, when $\tau = 0.001$. Increasing time steps strength of the cell increases and left hot cell shrinks in its size towards the hot thermally active location. Further increasing time, cold cell occupies the majority of the enclosure while hot cell shrinks. When $\tau = 0.05$, the cold and hot cells merging as a single cell with two secondary inner cells. When increasing time a single cell splitted into two cells in top and bottom of the enclosure, that is, one above another. Finally in the steady state top cell strengthen and grows in its size. The cell below of the enclosure is weakened and shrinks in its size. The iso-

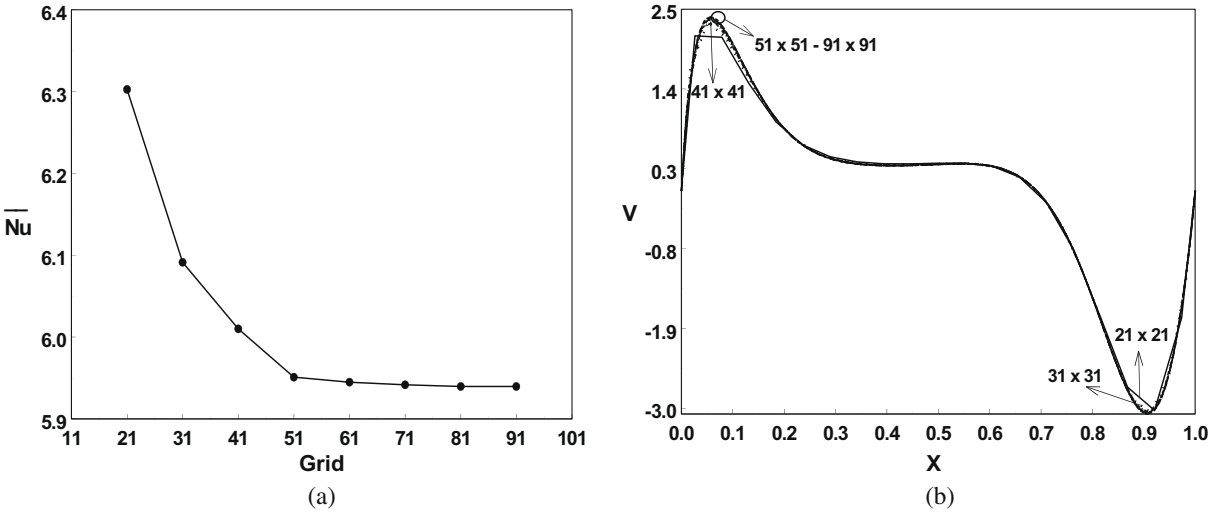

Fig. 2. (a–b) Average Nusselt number and velocity profile for different grid sizes, top heating active wall, $Pr = 11.573$, $Sc = 5$, $N = 1$, $R = D_f = S_r = 0$ and $Ra_T = 10^5$.

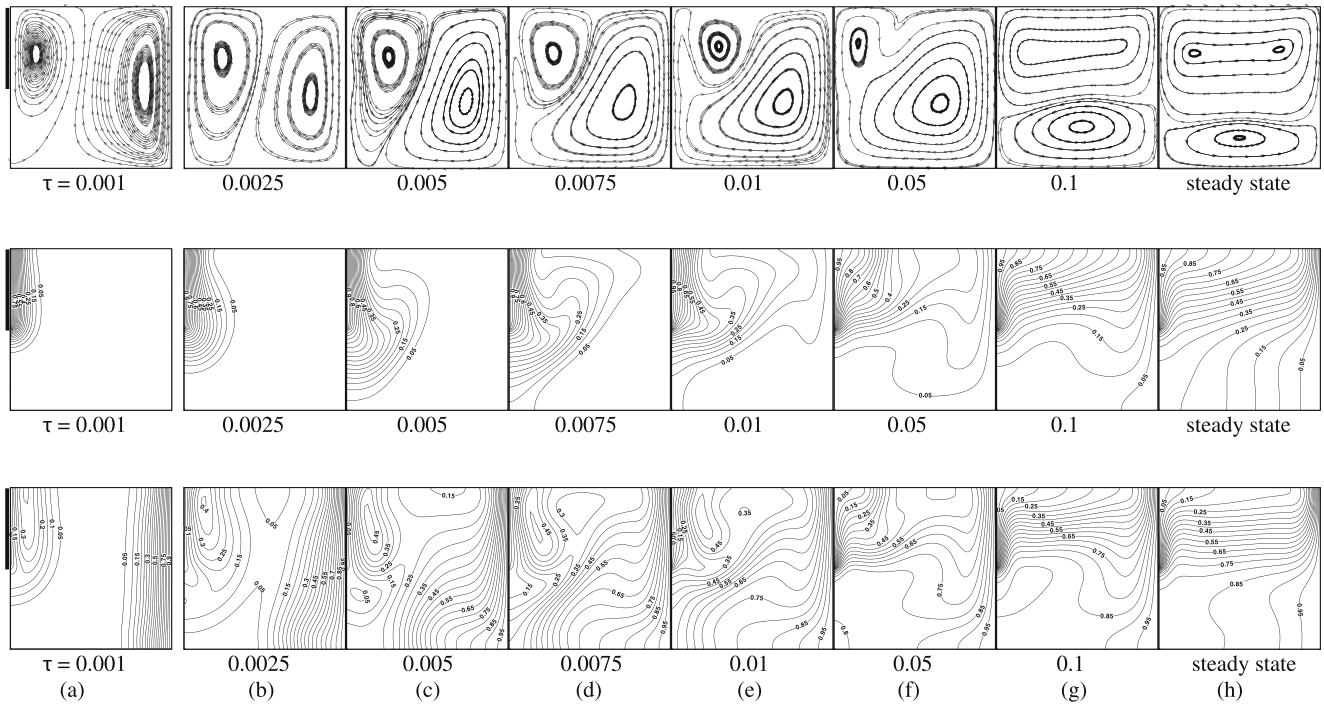

Fig. 3. (a–h) Transient state of streamlines, isotherms and iso-concentration for top heating active wall, case I, $R = 0.5$, $N = 1$, $Sc = 5$, $D_f = 0.0$, $S_r = 1.0$ and $Ra_T = 10^5$.

therms and iso-concentrations are almost parallel to the active parts indicating that only conduction mode of heat transfer is done for initial time steps. Increasing time, the temperature and concentration lines are spread out the whole enclosure and the convection is initiated. Further increasing time convection is dominated across the enclosure.

Fig. 4a–h illustrates the transient results of streamlines, isotherms and iso-concentrations for $Ra_T = 10^5$, $R = 0.5$, $N = 1$, $Sc = 5$, $S_r = 1.0$, $D_f = 0.0$ and for top heating active wall in case II. In the initial stage a small amount of fluid near the hot region is activated. For $\tau = 0.001$ a small counter clockwise rotating hot cell appears near the top heating location and the isotherms and iso-concentrations are almost parallel lines. They indicate conduction mode of heat transfer. At times $\tau = 0.0025$ and 0.005 the anti-clockwise rotating cell (developed from the cold wall as inversional convection) grows in size, moves slightly away from the boundary and expands, while the isotherms and iso-concentrations become parabolic and spreads to more than half of the enclosure. When $\tau = 0.0075$–0.05 the convective cell has moved to the center, elongated to elliptic shape and occupies the entire enclosure. The corresponding isotherms and iso-concentrations have reached the right side of the enclosure. As τ increases, the inner cell splits into two, the thermal boundary layer is well established showing the development of the convective mode of heat transfer.

The results are presented in terms of fluid flow, heat and mass transfer for different heating active walls (at top, middle and bottom left wall respectively), $R = 0.5$, $N = 1$, $Sc = 5$, $S_r = D_f = 0.5$ and $Ra_T = 10^5$ as seen in Fig. 5a–c (case I) and Fig. 6a–c (case II). In Fig. 5, the hot active region is along half portion of the left vertical wall at different location. In this figure we observe that the fluid

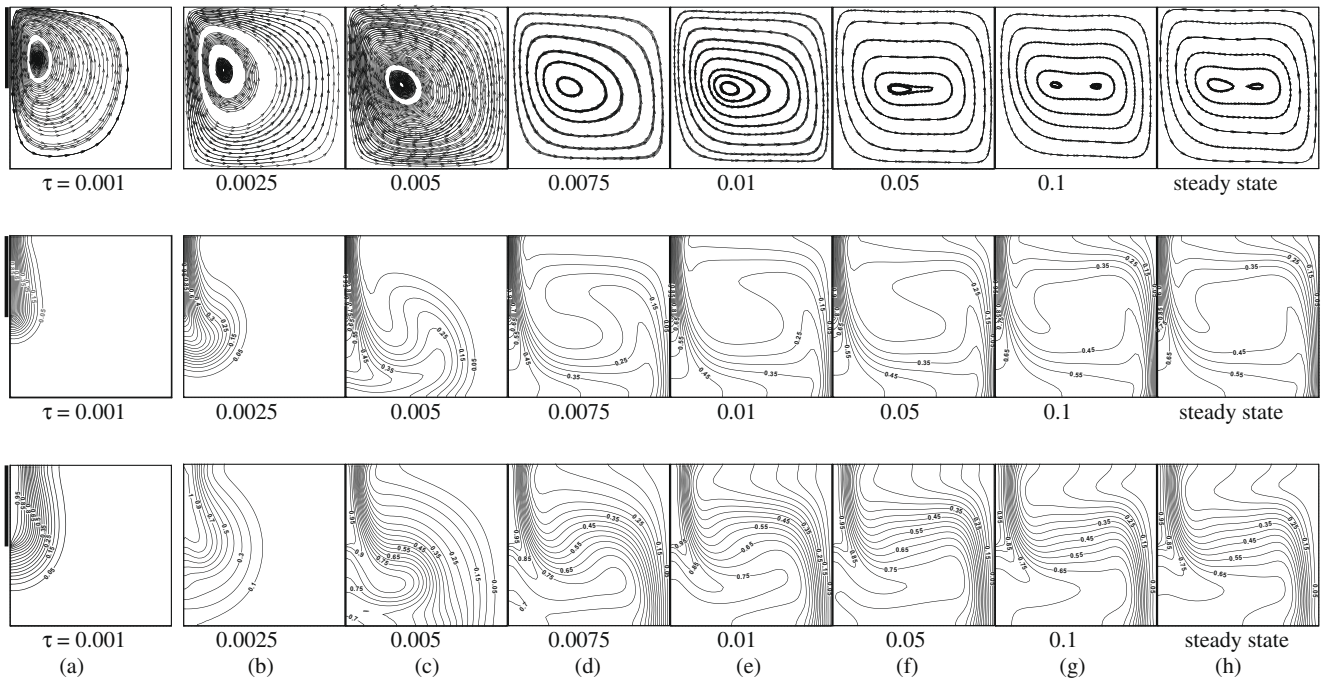

Fig. 4. (a–h) Transient state of streamlines, isotherms and iso-concentration for top heating active wall, case II, $R = 0.5$, $N = 1$, $Sc = 5$, $D_f = 0.0$, $S_r = 1.0$ and $Ra_T = 10^5$.

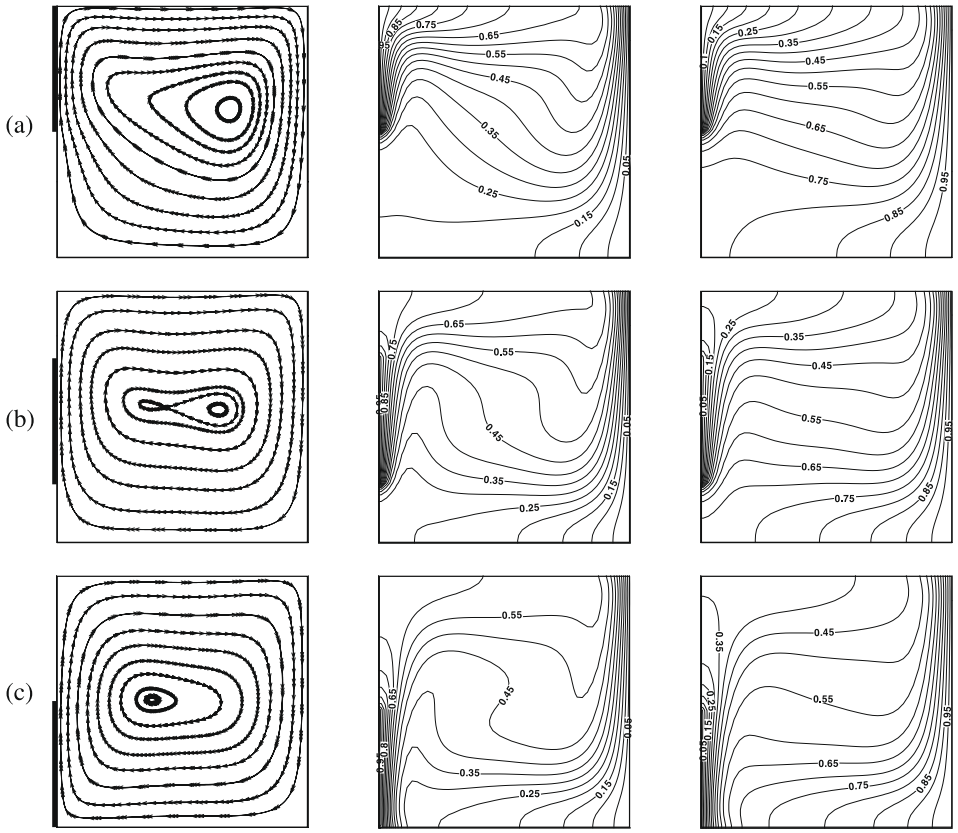

Fig. 5. (a–c) Steady state of streamlines, isotherms and iso-concentration for different heating active walls, case I, $R = 0.5$, $N = 1$, $Sc = 5$, $D_f = S_r = 0.5$ and $Ra_T = 10^5$.

flow covers the entire cavity. The fluid rises along the hot wall and falls along the right cold wall; this leads to formation of the thermal boundary layer at the upper part of the cold wall, the opposite reaction its hold as seen in Fig. 6. The isotherms and iso-concentrations are crowded around the active location on the left side of the enclosure. The core region of the convective cell is near the cold wall for top heating location and it moves to middle of the cell for middle heating location, then it comes to hot wall side for bottom heating location for case I in Fig. 5. The opposite behavior is observed for case II in Fig. 6.

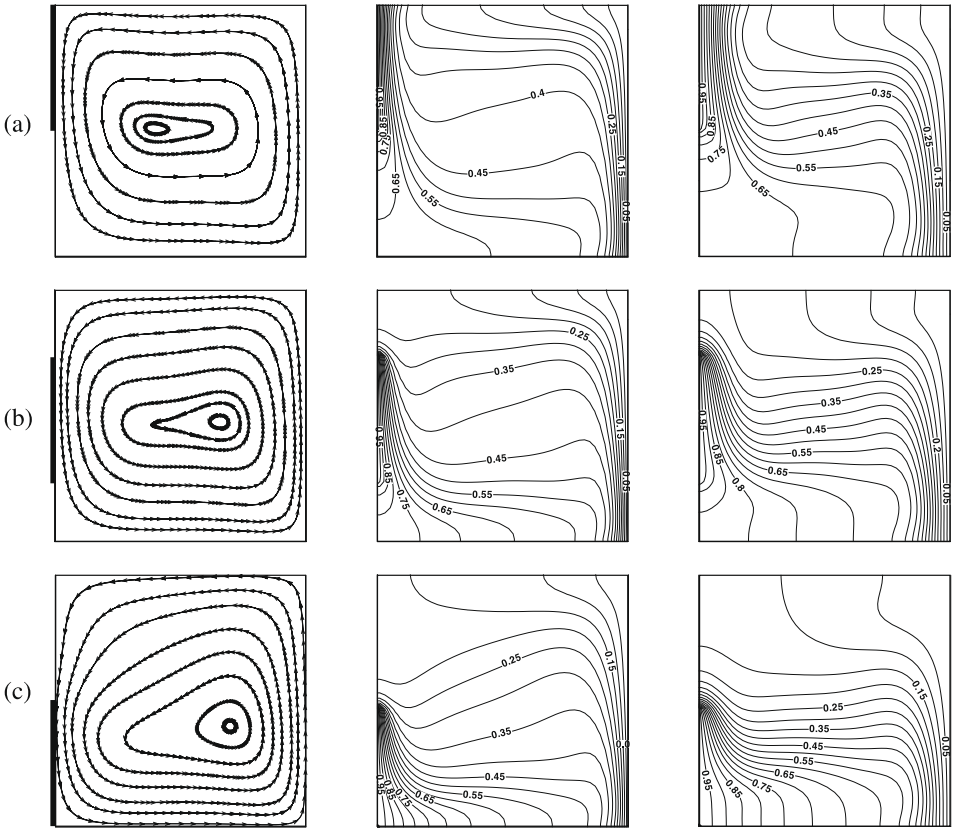

Fig. 6. (a–c) Steady state of streamlines, isotherms and iso-concentration for different heating active walls, case II, $R = 0.5$, $N = 1$, $Sc = 5$, $D_f = S_r = 0.5$ and $Ra_T = 10^5$.

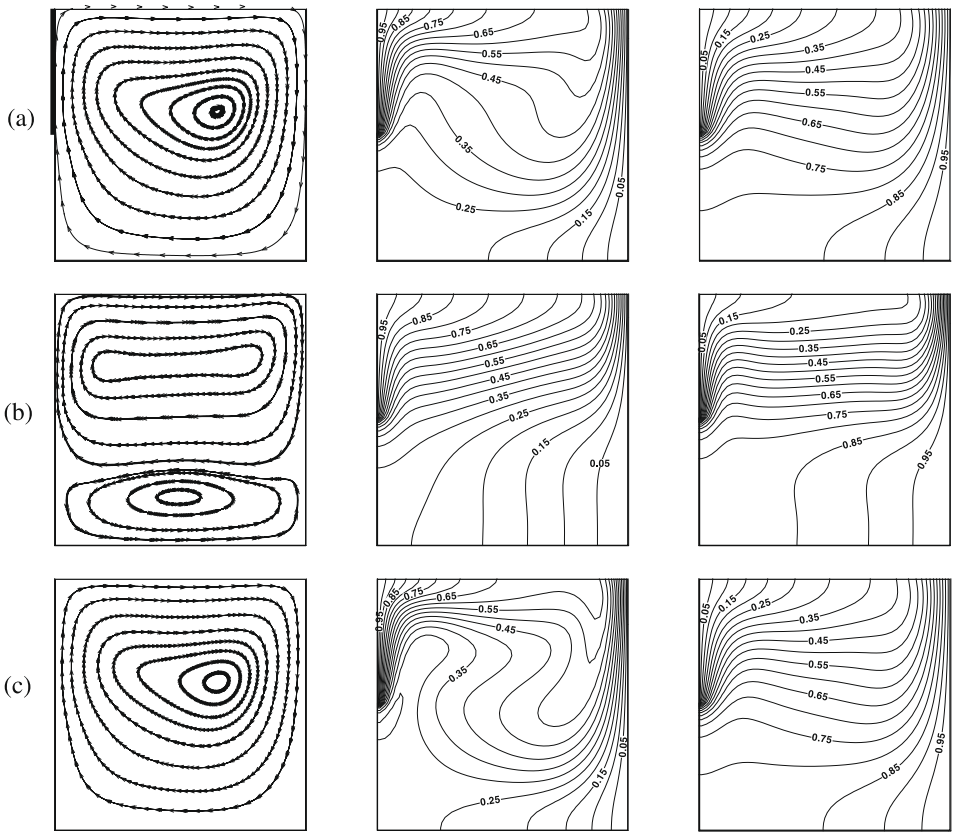

Fig. 7. (a–c) Steady state of streamlines, isotherms and iso-concentration for top heating active wall, case I, $R = 0.5$, $N = 1$, $Sc = 5$, and $Ra_T = 10^5$. (a) $D_f = 0.0$, $S_r = 0.0$, (b) $D_f = 0.0$, $S_r = 1.0$, (c) $D_f = 1.0$, $S_r = 0.0$.

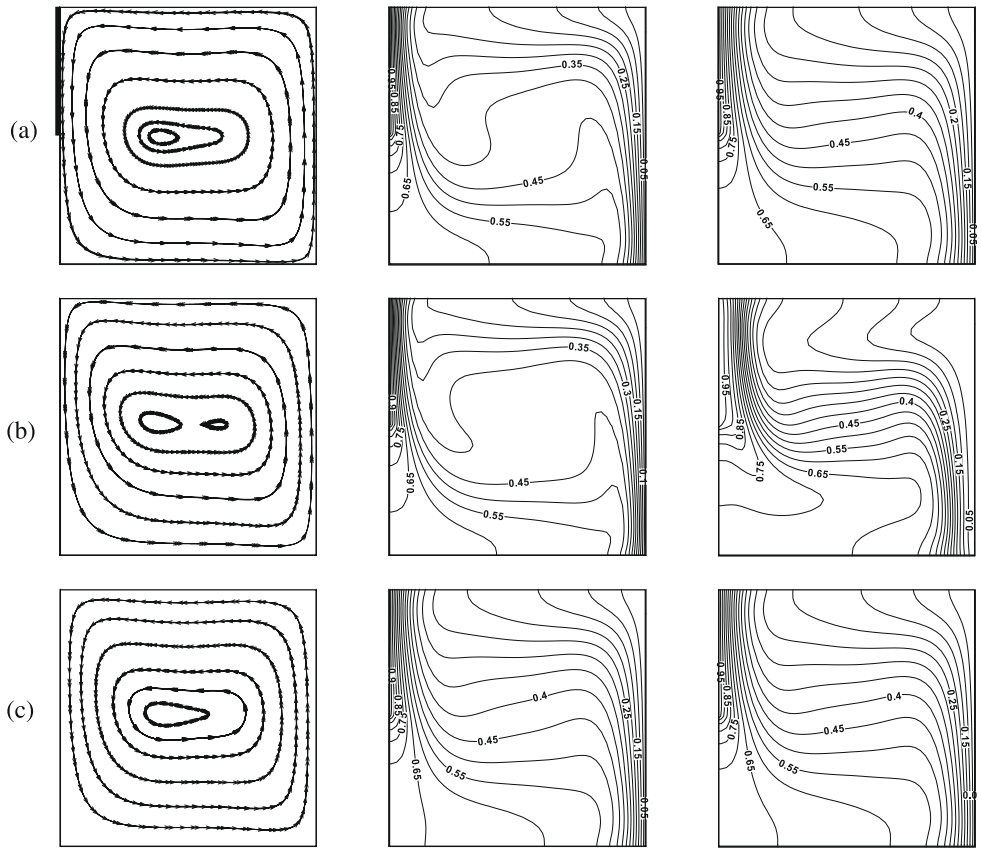

Fig. 8. (a–c) Steady state of streamlines, isotherms and iso-concentration for top heating active wall, case II, $R = 0.5$, $N = 1$, $Sc = 5$, and $Ra_T = 10^5$. (a) $D_f = 0.0$, $S_r = 0.0$, (b) $D_f = 0.0$, $S_r = 1.0$, (c) $D_f = 1.0$, $S_r = 0.0$.

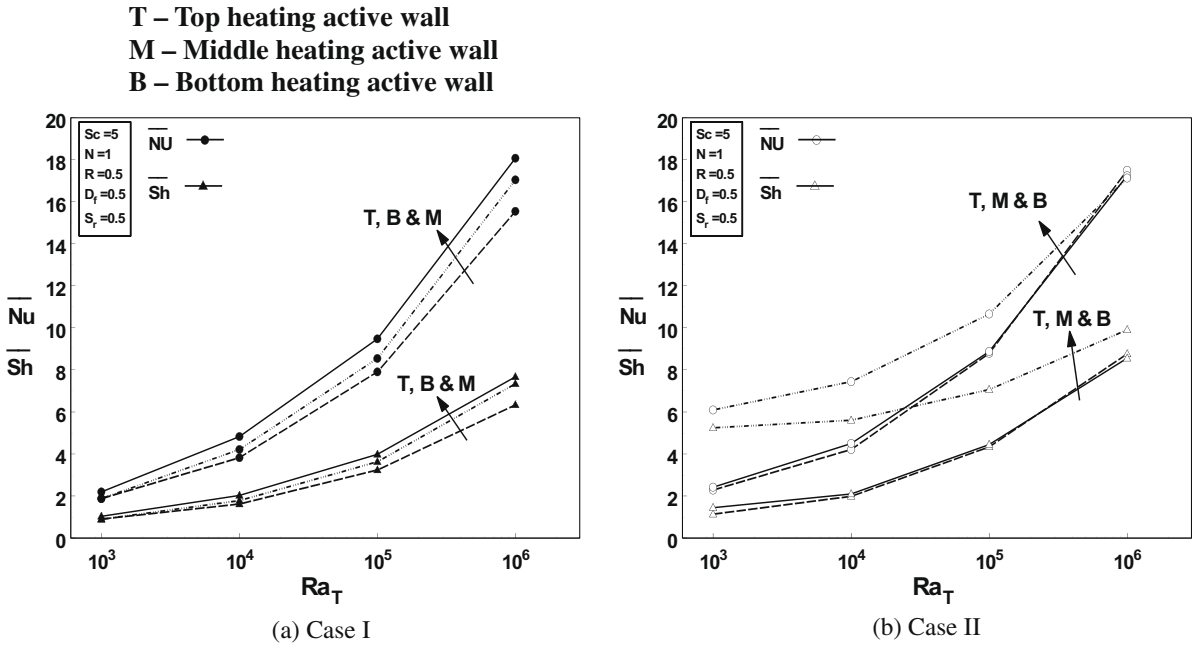

Fig. 9. (a–b) Average Nusselt number and Sherwood number vs thermal Rayleigh number for different heating active walls, $Sc = 5$, $N = 1$, $R = 0.5$, $D_f = S_r = 0.5$.

Figs. 7 and 8 show the effect of Soret and Dufour parameters on fluid flow, heat and mass transfer rates with top heating active location. In Fig. 7b, It is observed that the primary cell is pushed to the top of the enclosure and a weak cell rotating in anticlockwise direction is formed lower the primary cell at the bottom of the enclosure. The formation of the bi-cellular flow pattern reduces the heat transfer rate and increases the mass transfer. In the remaining cases unicellular flow is appeared for Fig. 7a and c. A single cell rotating in anti-clockwise direction appears inside the enclosure for case II in Fig. 8.

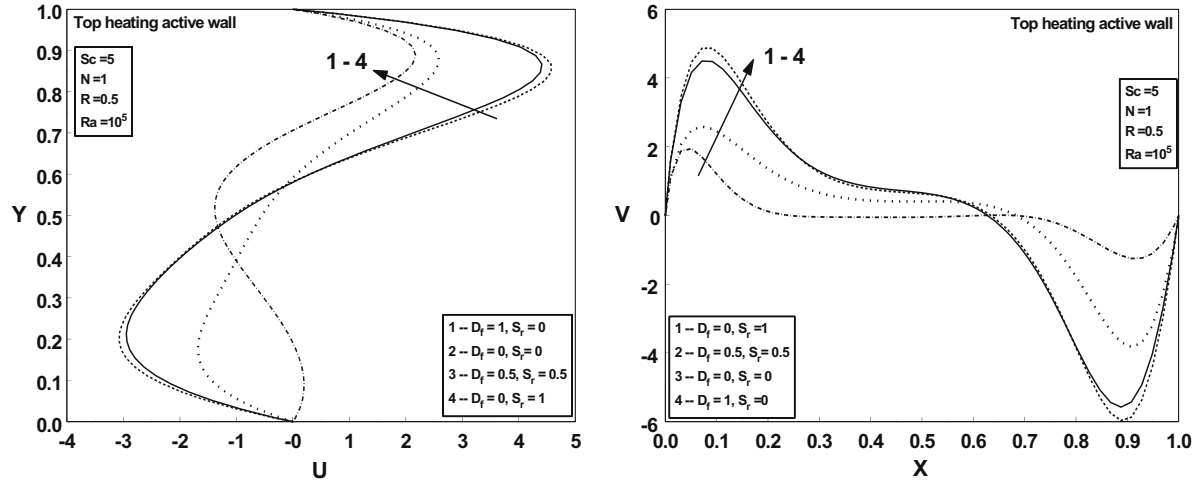

Fig. 10. (a–b) Mid-height horizontal and vertical velocities at the middle of the cavity for different Soret and Dufour numbers and case I.

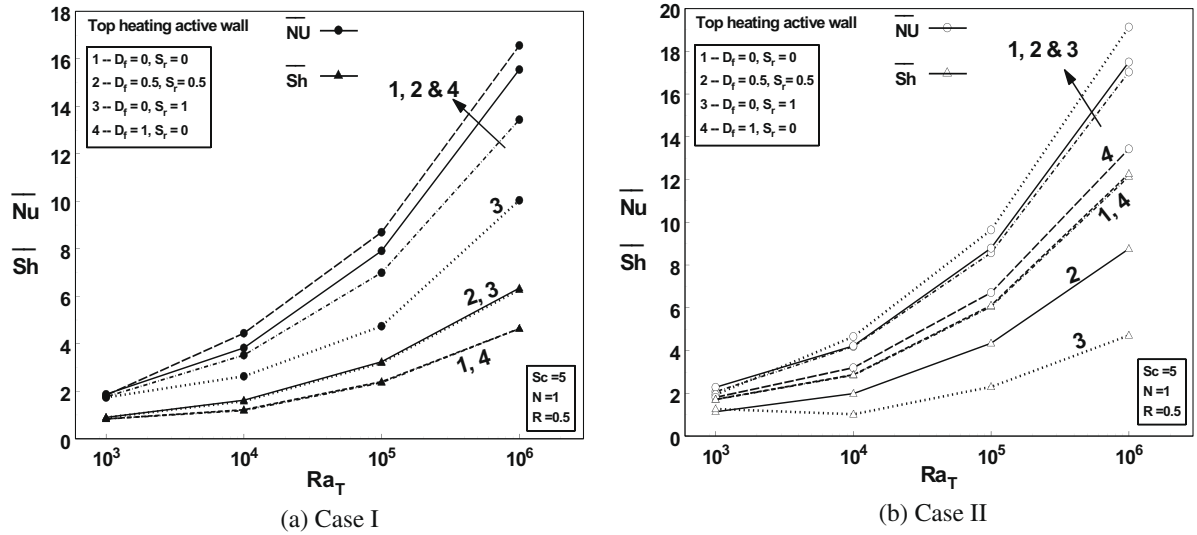

Fig. 11. (a–b) Average Nusselt number and Sherwood number vs thermal Rayleigh number for different D_f and S_r, $Sc = 5$, $N = 1$, $R = 0.5$.

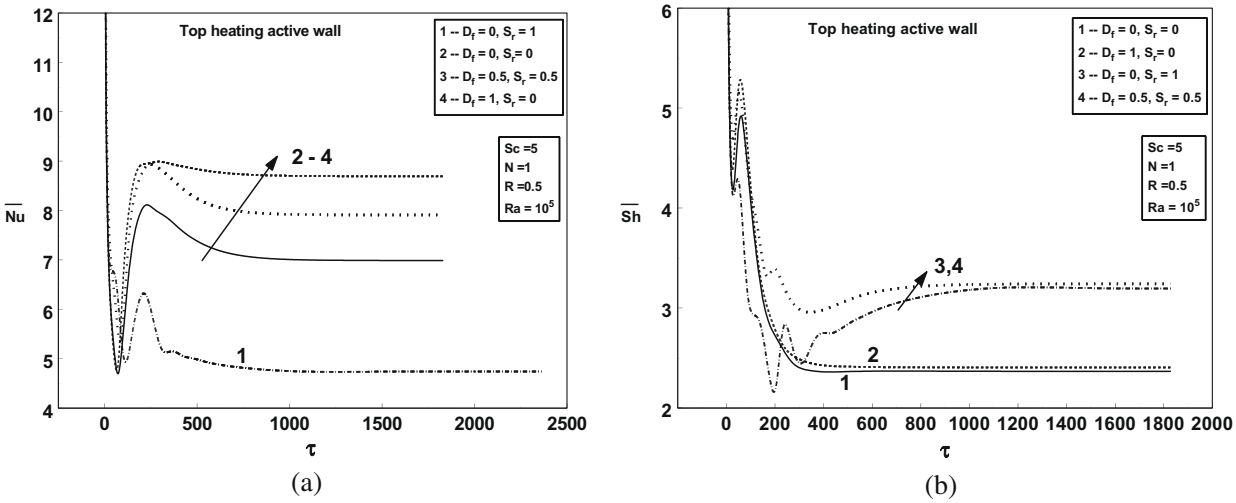

Fig. 12. (a–b) Average Nusselt number and Sherwood number vs. time τ for different D_f and S_r, top heating active wall, case I, $Sc = 5$, $N = 1$, $R = 0.5$ and $Ra_T = 10^5$.

The average Nusselt and Sherwood numbers are plotted as a function of thermal Rayleigh number for different thermally active walls in Fig. 9a and b. It is clear that, the heat and mass transfer rate is more for the middle heating location of the thermally active portion on the wall and much lower for the top heating active location for case I. But for the case II, the average Nusselt and Sherwood number is high for bottom active location. Top heating location gives poor heat and mass transfer rate as like case I.

Fig. 10a and b shows the mid-height horizontal and vertical profiles for the different Soret and Dufour effects. It is observed that the fluid particle moves with greater velocity for the high value of Dufour parameter and the velocity is very low for the presence of Soret parameter. The effect of heat and mass transfer rate against different thermal Rayleigh numbers and different Soret and Dufour coefficients with $Sc = 5$, $N = 1$ and $R = 0.5$ are shown in Fig. 11a and b. It is observed that the rate of heat and mass transfer increases when the values of thermal Rayleigh number increase. The heat transfer rate is high for $D_f = 1$, $S_r = 0$ while the mass transfer is also high for $D_f = 0$, $S_r = 1$ in case I. The opposite result of it holds in the case II.

The steady-state variations in average Nusselt and Sherwood numbers with respect to time for the top heating active position, $Ra_T = 10^5$, $R = 0.5$, $N = 1$, $Sc = 5$ and for different Soret and Dufour coefficients are shown in Fig. 12a–b. As time evolves the particles near the hot wall have higher temperature and so the heat and mass transfer rate starts decreasing, thus, we get a sudden fall in the values of average Nusselt and Sherwood numbers. Finally, the steady state is reached and tends to be constant.

5. Conclusions

A numerical model was employed to analyze the flow, heat and mass transfer of water filled in a partially heated active square enclosure with the presence of Soret and Dufour effects. The following conclusions are drawn. It is observed that the temperature of maximum density leaves strong effects on the heat and mass transfer due to the formation of bi-cellular structure. The non-linear behavior of heat and mass transfer rate is due to the maximum density effect. It is found that the rate of heat and mass transfer increases when the values of thermal Rayleigh number increase in all heating locations. The fluid particle moves with greater velocity and high heat transfer rate for the high value of Dufour coefficient and the velocity is less and high mass transfer rate for the presence of Soret coefficient in case I. The opposite behavior was observed for case II.

Acknowledgments

The authors gratefully acknowledge the support provided to this study by the NCKU Project of Promoting Academic Excellence.

References

Bahloul, A., Boutana, N., Vasseur, P., 2003. Double-diffusive and Soret-induced convection in a shallow horizontal porous layer. J. Fluid Mech. 491, 325–352.
Chang, W.J., Yang, D.F., 1995. Transient natural convection of water near its density extremum in a rectangular cavity filled with porous medium. Numer. Heat Trans. 28, 619–633.
Davis, D.V., 1983. Natural convection of air in a square cavity: a benchmark numerical solution. Int. J. Numer. Meth. Fluids 3, 249–264.
Erbay, B., Altac, Z., Sulus, B., 2004. Entropy generation in a square enclosure with partial heating from a vertical lateral wall. Heat Mass Trans. 40, 909–918.
Frederick, R.L., Quiroz, F., 2001. On the transition from conduction to convection regime in a cubical enclosure with a partially heated wall. Int. J. Heat Mass Trans. 44, 1699–1709.
Ho, C.J., Tu, F.J., 2001. Transition to oscillatory natural convection of water near its density maximum in a tall enclosure. Int. J. Numer. Methods Heat Fluid Flow 11, 626–641.
Joly, F., Vasseur, P., Labrosse, G., 2000. Soret-driven thermosolutal convection in a vertical enclosure. Int. Commun. Heat Mass Trans. 27, 755–764.
Kandaswamy, P., Sivasankaran, S., Nithyadevi, N., 2007. Buoyancy-driven convection of water near its density maximum with partially active vertical walls. Int. J. Heat Mass Trans. 50, 942–948.
Mansour, A., Amahmid, A., Hasnaoui, M., Bourich, M., 2006. Multiplicity of solutions induced by thermosolutal convection in a square porous cavity heated from below and submitted to horizontal concentration gradient in the presence of Soret effect. Num. Heat Trans. 49, 69–94.
Nansteel, M.W., Medjani, K., Lin, D.S., 1987. Natural convection of water near its density maximum in rectangular enclosure: low Rayleigh number calculations. Phys. Fluids 30, 312–317.
Nithyadevi, N., Kandaswamy, P., Sivasankaran, S., 2006. Natural convection in a square cavity with partially active vertical walls: time periodic boundary condition. Math. Prob. Eng. 2006, 1–16.
Nithyadevi, N., Kandaswamy, P., Lee, J., 2007. Natural convection in a rectangular cavity with partially active side walls. Int. J. Heat Mass Trans. 50, 4688–4697.
Nithyadevi, N., Yang, R.J., 2009. Magnetoconvection in an enclosure of water near its density maximum with Soret and Dufour effects. Int. J. Heat Mass Trans. 52, 1667–1676.
Osorio, A., Avila, R., Cervantes, J., 2004. On the natural convection of water near its density inversion in an inclined square cavity. Int. J. Heat Mass Trans. 47, 4491–4495.
Ostrach, A., 1988. Natural convection in enclosures. J. Heat Trans. 110, 1175–1190.
Oztop, H.F., 2007. Natural convection in partially cooled and inclined porous rectangular enclosures. Int. J. Thermal Sci. 46, 149–156.
Patankar, S.V., 1980. Numerical Heat Transfer and Fluid Flow. Hemisphere, McGraw-Hill, Washington, DC.
Patha, M.K., Murthy, P.V.S.N., Raja Sekhar, G.P., 2006. Soret and Dufour effects in a non-darcy porous medium. J. Heat Trans. 128, 605–610.
Platten, J.K., 2006. The Soret effect: a review of recent experimental results. J. Appl. Mech. 73, 5–15.
Sezai, I., Mohamad, A.A., 2000. Double diffusive convection in a cubic enclosure with opposing temperature and concentration gradients. Phys. Fluids 12, 2210–2223.
Sivasankaran, S., Kandaswamy, P., 2006. Double diffusive convection of water in a rectangular partitioned enclosure with temperature dependent species diffusivity. Int. J. Fluid Mech. Res. 33, 345–361.
Sivasankaran, S., Kandaswamy, P., 2007. Double diffusive convection of water in a rectangular partitioned enclosure with concentration dependent species diffusivity. J. Korean Soc. Industrial Appl. Math. 11, 71–83.
Tong, W., Koster, J.N., 1993. Coupling of natural convection flow across a vertical density inversion interface. Warme-und Stoffubertragung 28, 471–479.
Valencia, A., Frederick, R.L., 1989. Heat transfer in square cavities with partially active vertical walls. Int. J. Heat Mass Trans. 32, 1567–1574.
Yucel, N., Turkoglu, H., 1994. Natural convection in rectangular enclosures with partial heating and cooling. Warme-und Stoffubertragung 29, 471–478.